

# Dynamic tubulation of mitochondria drives mitochondrial network formation

Chong Wang<sup>1,4,\*</sup>, Wanqing Du<sup>1,4,\*</sup>, Qian Peter Su<sup>2,3,\*</sup>, Mingli Zhu<sup>1,4</sup>, Peiyuan Feng<sup>1,4</sup>, Ying Li<sup>1,4</sup>, Yichen Zhou<sup>5</sup>, Na Mi<sup>1,4</sup>, Yueyao Zhu<sup>1,4</sup>, Dong Jiang<sup>1,4</sup>, Senyan Zhang<sup>4</sup>, Zerui Zhang<sup>1,4</sup>, Yujie Sun<sup>2,3</sup>, Li Yu<sup>1,4</sup>

<sup>1</sup>State Key Laboratory of Biomembrane and Membrane Biotechnology, Tsinghua University-Peking University Joint Center for Life Sciences, School of Life Sciences, Tsinghua University, Beijing 100084, China; <sup>2</sup>State Key Laboratory of Membrane Biology, Biodynamic Optical Imaging Center (BIOPIIC), Beijing 100871, China; <sup>3</sup>School of Life Sciences, Peking University, Beijing 100871, China; <sup>4</sup>School of Life Sciences, Tsinghua University, Beijing 100084, China; <sup>5</sup>Mathematical Science Center, Tsinghua University, Beijing 100084, China

**Mitochondria form networks. Formation of mitochondrial networks is important for maintaining mitochondrial DNA integrity and interchanging mitochondrial material, whereas disruption of the mitochondrial network affects mitochondrial functions. According to the current view, mitochondrial networks are formed by fusion of individual mitochondria. Here, we report a new mechanism for formation of mitochondrial networks through KIF5B-mediated dynamic tubulation of mitochondria. We found that KIF5B pulls thin, highly dynamic tubules out of mitochondria. Fusion of these dynamic tubules, which is mediated by mitofusins, gives rise to the mitochondrial network. We further demonstrated that dynamic tubulation and fusion is sufficient for mitochondrial network formation, by reconstituting mitochondrial networks *in vitro* using purified fusion-competent mitochondria, recombinant KIF5B, and polymerized microtubules. Interestingly, KIF5B only controls network formation in the peripheral zone of the cell, indicating that the mitochondrial network is divided into subzones, which may be constructed by different mechanisms. Our data not only uncover an essential mechanism for mitochondrial network formation, but also reveal that different parts of the mitochondrial network are formed by different mechanisms.**

**Keywords:** dynamic tubulation; KIF5B; mitochondrial network; mitochondrial fusion

*Cell Research* (2015) 25:1108-1120. doi:10.1038/cr.2015.89; published online 24 July 2015

## Introduction

Formation and maintenance of the mitochondrial network play an important role in maintaining mitochondrial functions. Destruction of the mitochondrial network affects mitochondrial DNA integrity, interchange of mitochondrial material, respiratory capacity, apoptosis, and response to cellular stress, leading to the abnormal development and several human diseases including neurodegenerative disease [1, 2].

In the current view, the mitochondrial network is

formed by fusion of individual mitochondria, and the balance between fusion and fission determines the overall mitochondrial morphology [3], which can change dramatically in response to cell cycle, intracellular energy levels and cellular stresses [4]. Cells with a high fusion-to-fission ratio have long, tubular mitochondria and a highly interconnected mitochondrial network; conversely, cells with a low fusion-to-fission ratio have fragmented mitochondria, which appear as spheres or short rods [5-8]. So far, mitofusin 1 (Mfn1) and mitofusin 2 (Mfn2) have been identified as core components of the machinery for mitochondrial fusion in mammals [9, 10]. In mitofusin-defective cells, the mitochondrial network is completely disrupted and the mitochondria become spheres or short rods. However, fusion of individual mitochondria is not sufficient to form mitochondrial networks *in vitro* [11], indicating that other unknown mechanisms are essential for mitochondrial network for-

\*These three authors contributed equally to this work.

Correspondence: Li Yu<sup>a</sup>, Yujie Sun<sup>b</sup>

<sup>a</sup>E-mail: liyulab@mail.tsinghua.edu.cn

<sup>b</sup>E-mail: sun\_yujie@pku.edu.cn

Received 12 February 2015; revised 10 May 2015; accepted 5 June 2015; published online 24 July 2015

mation.

The basic module for network formation is the tubule. Tubules connect to form a lattice, and the network is a series of interconnected lattices. Hypothetically, a network can be constructed by pulling tubules out of existing membrane compartments and then connecting these tubules by fusion to give a lattice; by repeating this process, a network can be created.

Kinesins (KIFs) are microtubule-based motor proteins that move along microtubule filaments [12]. Using the force generated, KIF proteins move organelles along microtubules. KIF proteins can also induce membrane tubulation *in vitro* by pulling the membrane [13, 14]. KIF5B, a member of Kinesin 1 family, has been shown to play important roles in transporting mitochondria and maintaining mitochondrial distribution [15]. In KIF5B-knockout cells, mitochondrial distribution is disrupted and mitochondria accumulate in the perinuclear region. These observations prompted us to hypothesize that kinesin-driven tubulation of mitochondria may play an important role in formation of mitochondrial networks.

In this study, we report a new mechanism for formation of mitochondrial networks. We observed that thin tubules are rapidly extended from and retracted by mitochondria, a process we named as dynamic tubulation. We demonstrated that KIF5B drives dynamic tubulation. In *KIF5B*<sup>-/-</sup> cells, the mitochondrial network shrinks to the perinuclear area, and the peripheral zone of the cell is completely devoid of mitochondria. Restoration of KIF5B expression in these cells causes dynamic tubulation of mitochondria, and subsequent fusion of these dynamic tubules leads to network formation in the peripheral zone of the cell. Furthermore, we successfully reconstituted mitochondrial networks *in vitro* using purified fusion-competent mitochondria, recombinant KIF5B and polymerized microtubules. Our data not only establish dynamic tubulation of mitochondria driven by KIF5B as an essential mechanism for mitochondrial network formation, but also reveal that different parts of the mitochondrial network are formed by different mechanisms.

## Results

### *Dynamic tubulation of mitochondria*

Structured illumination microscopy (SIM) reveals thin tubules extending from mitochondria (Figure 1A). These tubules are hard to capture by regular transmission electron microscopy (TEM), but are regularly observed by high-pressure freezing TEM (Figure 1B). Time-lapse imaging reveals that these tubules are highly dynamic; they are rapidly extended from and retracted by mitochondria with an average life span of 11 s (Supplementary infor-

mation, Figure S1). Their duration varies greatly, with some tubules lasting more than 40 s (Figure 1C, Supplementary information, Movies S1 and S2). We named the tubules as “dynamic tubules” and the process as “dynamic tubulation”. The dynamic tubulation of mitochondria is very similar to nanotunneling in mitochondria from cardiomyocytes [16]. These “dynamic” tubules are different from regular tubular mitochondria, as the latter are much thicker and more static (Supplementary information, Figure S1). Although the dynamic tubules are very thin, they do contain mitochondrial matrix (Figure 1D). These tubules are aligned with microtubules (Figure 1E and Supplementary information, Movie S3), and disruption of microtubules can completely block dynamic tubulation (Figure 1F and Supplementary information, Figure S2). Dynamic tubulation of mitochondria appears to be a common phenomenon, as it was observed in all the cell lines we tested (Figure 6F and Supplementary information, Figure S3). Although many dynamic tubules are retracted back without obvious consequence, we observed that some of the tubules fuse with other mitochondria to form a membrane bridge between two mitochondria (Figure 1G and Supplementary information, Figures S1, S4 and Movie S4). These membrane bridges quickly thicken and become part of the mitochondrial network (Figure 1G and Supplementary information, Movie S4). This observation prompted us to study the role of dynamic tubulation in formation of the mitochondria network.

### *KIF5B drives dynamic tubulation*

It is well established that in KIF5B-knockout cells, mitochondrial distribution is disrupted and mitochondria accumulate in the perinuclear region [15]. Thus, KIF5B-knockout cells could be a useful tool to test our hypothesis. We reasoned that if we put KIF5B back into KIF5B-knockout cells in a controlled fashion, and analyze how the mitochondrial network is restored, we should be able to reveal how KIF5B regulates mitochondria network formation. First, we used CRISPR/Cas to knock out KIF5B in normal rat kidney cells (NRK) that stably express Mito-YFP (Figure 2A). In agreement with the existing literature [15], mitochondria accumulate in the perinuclear region, which occupies roughly 47% of the cell cytoplasm (Figure 2B and 2C). The outer regions of the cell are completely devoid of mitochondria. It is worth noting that the perinuclear mitochondria still form networks (Figure 2B), indicating that mitochondrial network formation in the perinuclear area is independent of KIF5B.

Next, we stably expressed TET-ON KIF5B in the KIF5B-knockout NRK cells (Figure 2D). As a control, we also stably expressed KIF5B T92N (Figure 2E), a mutant KIF5B that lacks mobility [17]. Adding tetracy-

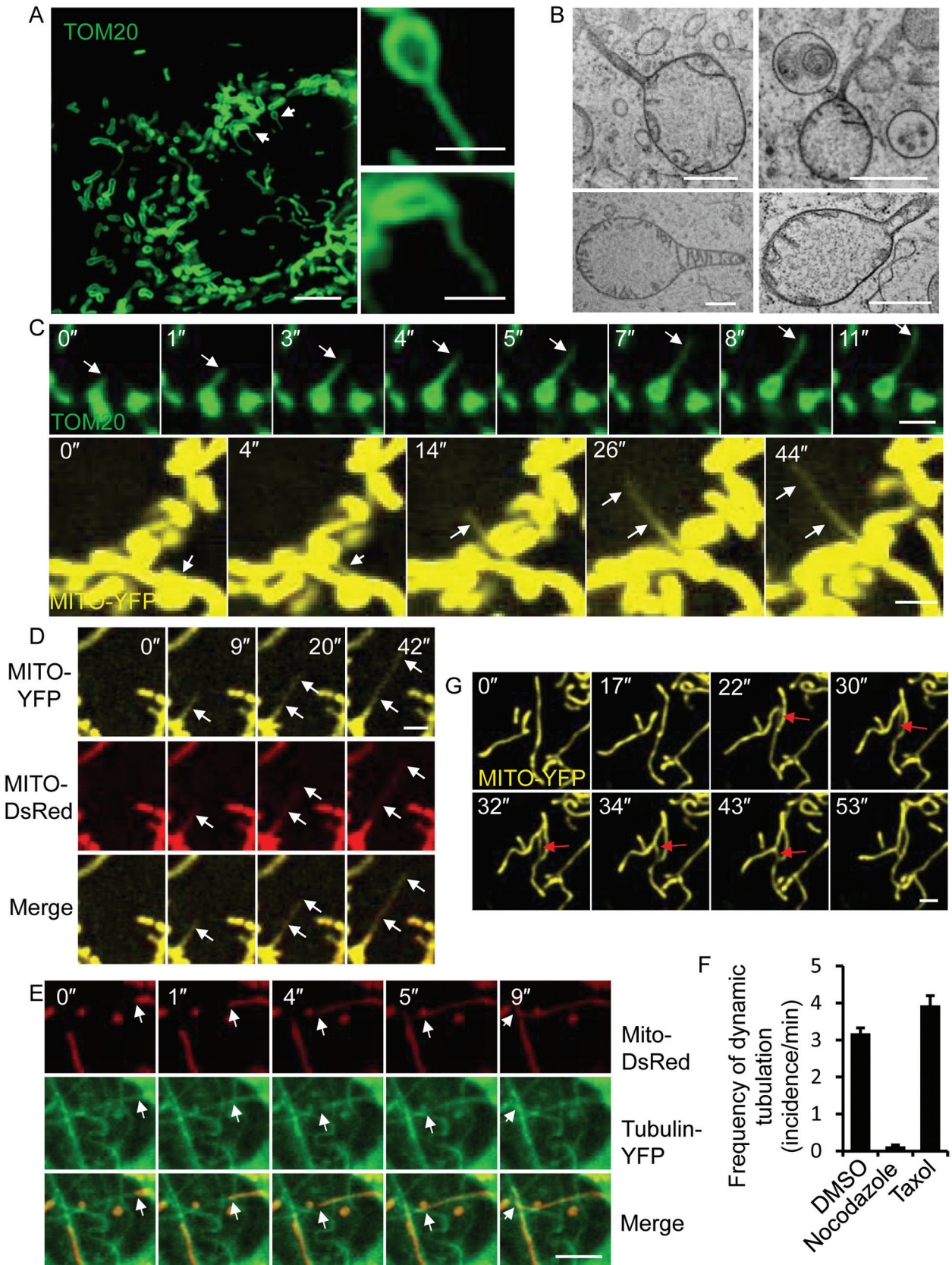


**Figure 1** Dynamic tubulation of mitochondria. **(A)** NRK cells stably expressing the mitochondrial marker TOM20-GFP were visualized by N-SIM microscopy. Scale bar, 5  $\mu\text{m}$ . Structures indicated by the white arrows are enlarged in the right-hand panels. Scale bar in enlarged panels, 1  $\mu\text{m}$ . **(B)** NRK cells were observed by high-pressure freezing TEM. Scale bar, 0.5  $\mu\text{m}$ . **(C)** NRK cells stably expressing the mitochondrial markers TOM20-GFP (top) or Mito-YFP (bottom) were visualized by spinning-disk microscopy. Scale bar, 2  $\mu\text{m}$ . White arrows indicate the tubulation process. **(D)** Mito-YFP-expressing NRK cells were transfected with the mitochondrial matrix marker Mito-DsRed, and then observed by spinning-disk microscopy. Scale bar, 2  $\mu\text{m}$ . White arrows indicate dynamic tubules. **(E)** NRK cells were transfected with Mito-DsRed and Tubulin-YFP, and then observed by spinning-disk microscopy. Scale bar, 5  $\mu\text{m}$ . White arrows indicate the tubulation process. **(F)** Frequency of dynamic tubulation in NRK cells treated with DMSO, nocodazole or taxol was quantified.  $n = 90$  cells from three independent experiments. Error bars indicate SD. **(G)** NRK cells stably expressing Mito-YFP were visualized by spinning-disk microscopy. Scale bar, 2  $\mu\text{m}$ . Red arrows indicate a tubulation event that mediates fusion of two mitochondrial tubules.

cline induces expression of KIF5B and restores the mitochondrial network in 4 h (Figure 2F and Supplementary information, Figure S5). In contrast, tetracycline-induced expression of KIF5B T92N failed to restore the mitochondrial network (Figure 2F), indicating that mobility of KIF5B is required for mitochondrial network formation. Similarly, adding nocodazole completely blocked the TET-ON KIF5B-mediated restoration of the mitochondrial network (Figure 2F).

Using this system, we analyzed how KIF5B controls formation of mitochondrial networks in the peripheral zone of cells. We found that restoration of mitochondrial distribution takes place in three stages (Figure 3A). During stage 1, tubular structures extend outward from the periphery of the perinuclear mitochondrial network (0-1 h). Stage 2 involves formation of lattices in the cell periphery (2-4 h). In stage 3, the mitochondrial network is restored (after 4 h). It is worth noting that although every cell will go through these stages, the exact timing varies considerably for individual cells.

Next, we monitored the outwardly-extending tubules during stage 1 at higher temporal resolution. We noticed that these outwardly-projecting tubules are very similar to the dynamic tubules that we observed in wild-type cells. They are highly dynamic, oscillate back and forth (Figure 3B and Supplementary information, Movie S5), and repeatedly change direction (Supplementary information, Figure S6, top row; Movie S6). In some cases these tubules branch out from existing mitochondrial tubules (Supplementary information, Figure S6, bottom row; Movie S7). These tubules are markedly thinner than mitochondrial tubules in an established network. Labeling with the fluorescent mitochondrial matrix marker Mito-DsRed revealed that mitochondrial matrix is present inside these dynamic, thin tubules (Supplementary information, Figure S7). In contrast, there are very few, if any, outwardly-projecting tubules in control cells that were not treated with tetracycline (Figure 3C, Supplementary information, Figure S8 and Movie S8). Similarly, no outwardly-projecting tubules were observed when expres-

sion of KIF5B T92N was induced or when expression of KIF5B was induced in the presence of nocodazole (Figure 3C). Thus, we conclude that in our experimental setting, mitochondria undergo KIF5B-mediated dynamic tubulation, which gives rise to dynamic tubules that radiate outward from the periphery of the mitochondrial network.

The dynamic tubules are abundant and change direction freely, frequently touching each other. In the majority of cases this results in fusion of two tubules at the connecting point (Figure 3D and Supplementary information, Movie S9). Once fused, the dynamic tubules are stabilized, and soon become thickened (Supplementary information, Movies S9 and S10), suggesting that the dynamic tubules become regular mitochondrial tubules after fusion, possibly by lateral movement of the membrane. Fusion of two dynamic tubules, which may come from the same or different mitochondrial tubule(s), gives rise to a triangular (Figure 3D) or quadrilateral lattice (Supplementary information, Figure S9), resulting in outward expansion of the mitochondrial network. Although at this stage the lattices are much more stable than the highly dynamic tubules, they are still less stable than established mitochondrial networks in the perinuclear region.

Next, we analyzed the dynamics of stage 2. At the start of stage 2, a loose mitochondrial network has already taken shape. The tubular lattices still retain a high degree of dynamic activity. Although it is relatively rare to see a lattice break up, the shape and location of the lattices keep changing (Supplementary information, Figure S9 and Movie S11). During stage 2, dynamic tubules still form at high frequency. Most of them will connect with a mitochondrial tubule within the same lattice or a different lattice (Figure 3E, Supplementary information, Movies S11 and S12), resulting in formation of an intra-lattice or inter-lattice membrane bridge. Similar to stage 1, the fusion of dynamic tubules with other mitochondrial tubules results in tubule thickening. Gradually, this process leads to a denser, more stable network composed of smaller lattices. By the end of stage 2, the mitochondrial network looks very similar to that in a normal cell (Figure 3A).

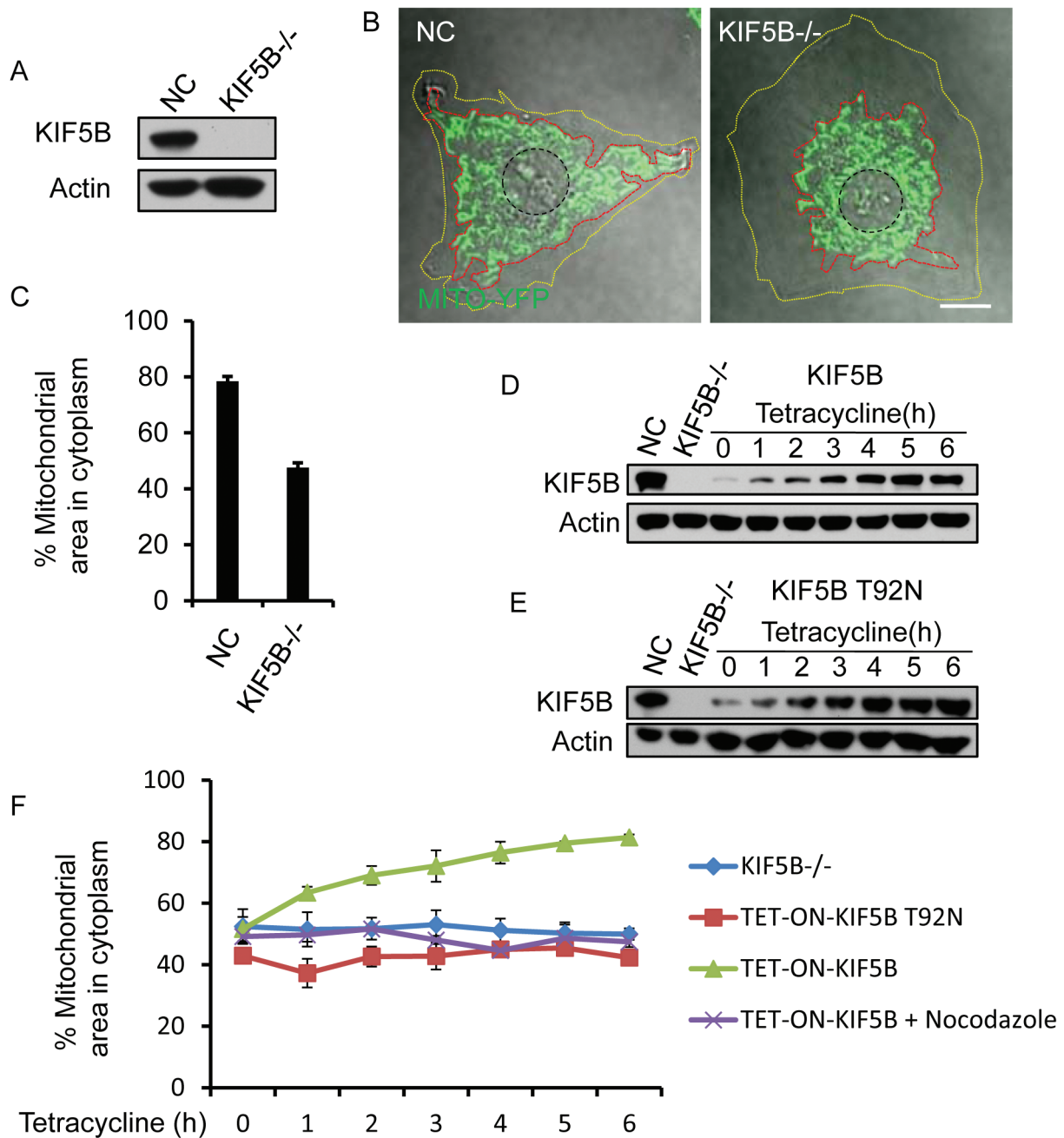


**Figure 2** KIF5B drives peripheral mitochondrial network formation. **(A)** CRISPR/Cas-mediated knockout of KIF5B in NRK cells stably expressing Mito-YFP. Expression levels of KIF5B were examined by western blotting. **(B)** Control and KIF5B-knockout cells were observed by confocal microscopy. Yellow dashed lines indicate the cell boundary; red dashed lines indicate the boundary of the mitochondrial network; and black dashed lines indicate the boundary of nucleus. Scale bar, 10  $\mu$ m. **(C)** The cytoplasmic area occupied by mitochondria was quantified in  $n = 90$  cells from three independent experiments. Error bars indicate SD. **(D)** KIF5B<sup>-/-</sup> NRK cells that stably express Mito-YFP and TET-ON-KIF5B were treated with 0.5  $\mu$ g/ml tetracycline. KIF5B induction was monitored by western blotting. **(E)** KIF5B<sup>-/-</sup> NRK cells that stably express Mito-YFP and TET-ON-KIF5B T92N were treated with 0.5  $\mu$ g/ml tetracycline. KIF5B T92N induction was monitored by western blotting. **(F)** Quantification of the area occupied by mitochondria in KIF5B<sup>-/-</sup> NRK cells, TET-ON-KIF5B T92N cells, TET-ON-KIF5B cells, and TET-ON-KIF5B cells pretreated with 5  $\mu$ g/ml nocodazole.  $n = 90$  cells from three independent experiments. Error bars indicate SD.

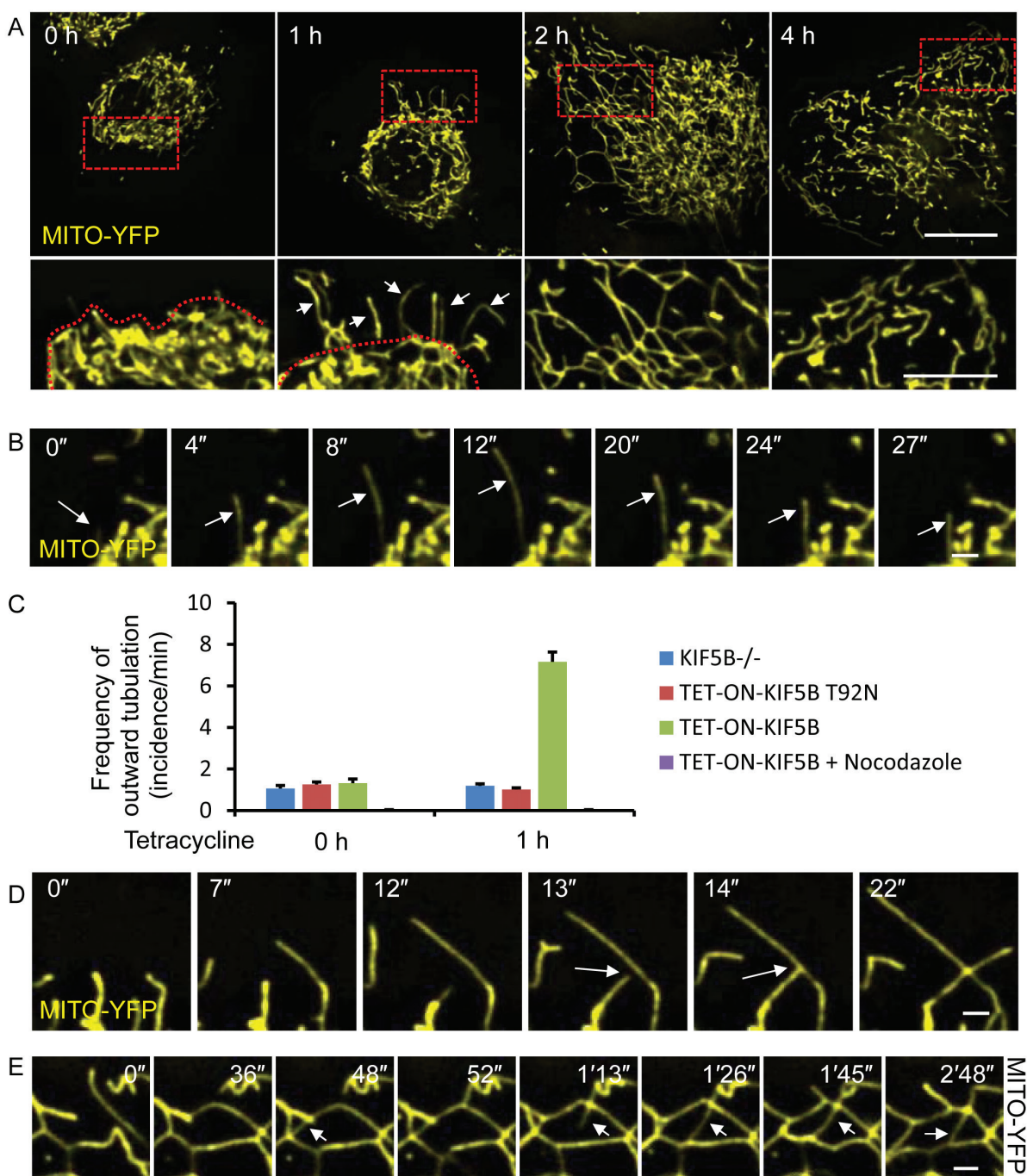


**Figure 3** KIF5B drives peripheral mitochondrial network formation in three steps. **(A)** *KIF5B*<sup>-/-</sup> NRK cells that stably express Mito-YFP and TET-ON-KIF5B were treated with 0.5  $\mu$ g/ml tetracycline, and then observed by spinning-disk microscopy. Scale bar, 20  $\mu$ m. Red dashed boxes are enlarged in the lower panels. Red dashed lines in the lower panels indicate the boundary of the mitochondrial network before tubulation, and white arrows indicate dynamic tubules. Scale bar in enlarged panels, 10  $\mu$ m. **(B)** *KIF5B*<sup>-/-</sup> NRK cells that stably express Mito-YFP and TET-ON-KIF5B were treated with 0.5  $\mu$ g/ml tetracycline for 1 h, and then observed by spinning-disk microscopy. Scale bar, 2  $\mu$ m. White arrows indicate a dynamic tubule. **(C)** Quantification of the frequency of outward tubulation from the mitochondrial boundary. *n* = 90 cells from three independent experiments. Error bars indicate SD. **(D)** *KIF5B*<sup>-/-</sup> NRK cells that stably express Mito-YFP and TET-ON-KIF5B were treated with 0.5  $\mu$ g/ml tetracycline for 1 h. Cells were observed by spinning-disk microscopy. Scale bar, 2  $\mu$ m. White arrows indicate a fusion event. **(E)** *KIF5B*<sup>-/-</sup> NRK cells that stably express Mito-YFP and TET-ON-KIF5B were treated with 0.5  $\mu$ g/ml tetracycline for 2 h. Cells were observed by spinning-disk microscopy. Scale bar, 2  $\mu$ m. White arrows indicate dynamic tubules.

These observations suggested that KIF5B is necessary for distribution of the mitochondrial network to the cell periphery, and KIF5B causes the outward expansion of the mitochondrial network by pulling dynamic tubules out of the mitochondria and then fusing them into lattices.

#### *KIF5B drives dynamic tubulation in vitro*

Next, to test whether KIF5B-mediated tubulation is sufficient to make a mitochondrial network, we set up an *in vitro* reconstitution system. First, we purified full-length KIF5B using the baculovirus expression system (Figure 4A) and checked its motor activity using a gliding assay (Supplementary information, Movie S13). As a control, we also purified full-length KIF5B T92N (Supplementary information, Figure S10 and Movie S14). Since KIF5B is co-localized with mitochondria *in vivo* (Figure 4B) and KIF5B has the same distribution pattern as mitochondria in a density gradient (Figure 4C), we hypothesized that KIF5B can be recruited to mitochondria *in vitro*. We isolated mitochondria from rat liver by density gradient centrifugation (Figure 4D). When we incubated full-length KIF5B or GST with purified mitochondria, we found that KIF5B, but not GST, can be pulled down by the mitochondria (Figure 4E). We also used Atto550-labeled KIF5B to verify by fluorescence microscopy that KIF5B is recruited to the surface of purified mitochondria (Figure 4F).

Next, we tested whether the association between KIF5B and purified mitochondria is sufficient to pull tubules out of the mitochondria. First, full-length KIF5B was incubated with purified mitochondria, then the mixture was transferred to a microtubule-coated glass chamber, and pulling was triggered by adding ATP (Figure 5A). We found that in the presence of ATP, KIF5B and microtubules, at least 30% of mitochondria form tubules, whereas no tubules were formed in the absence of ATP or microtubules or when KIF5B was replaced by KIF5B T92N (Figure 5B). The tubules are aligned with microtubules (Figure 5C and Supplementary information, Movie S15), and they are not stable; instead, they oscillate back and forth (Figure 5D and Supplementary information, Movie S16). Immunostaining using a TOM20 antibody confirmed that these structures are mitochondrial tubules (Figure 5E). Scanning electron microscopy revealed that the diameter of the mitochondrial tubules pulled out by KIF5B is around 100 nm (Figure 5F). These data suggest that KIF5B can indeed pull dynamic tubules out of mitochondria.

#### *KIF5B and mitofusins drive mitochondrial network reformation in vitro*

Next, we tested whether the tubules generated in our

*in vitro* system can form a network. We reasoned that if numerous tubules can be made simultaneously, a network may be produced. When we increased the concentration of mitochondria in the reaction and triggered tubulation with ATP, we observed that a mitochondrial network indeed formed (Figure 6A and 6B; Supplementary information, Movie S17). Time-lapse images revealed that mitochondrial network formation followed a pattern similar to that *in vivo*. First, tubules fuse to form lattices (Figure 6C, top row; Supplementary information, Movie S18), and then tubules form bridges between the strands of the lattices (Figure 6C, middle row; Supplementary information, Movie S19). Finally, tubules are pulled from the outer edge of the newly formed lattices, causing an outward expansion of the mitochondrial network (Figure 6C, bottom row; Supplementary information, Movie S20).

It is well known that mitochondrial fusion is mediated by Mfn1 and Mfn2 [9, 10]. In agreement with existing literature, the mitochondrial network is completely disrupted in cells that are null for both Mfn1 and Mfn2 (Mfn-null MEF cells; Figure 6D and 6E), and mitochondria are present in the form of round or oval-shaped vesicles. In Mfn-null MEF cells, dynamic tubulation can still occur (Figure 6F and Supplementary information, Movie S21), but the tubules fail to fuse into networks. Next, we purified mitochondria from wild-type or Mfn-null MEF cells. KIF5B can still pull tubules out of Mfn-null mitochondria; however, the formation of networks *in vitro* is completely abolished (Figure 6G and Supplementary information, Figure S11). Moreover, high-resolution time-lapse imaging reveals that tubulation of mitochondria from Mfn-null MEF cells is non-productive. The tubules keep oscillating back and forth, and connection of two tubules fails to cause fusion (Figure 6H and Supplementary information, Movie S22), therefore a network is never formed. In contrast, dynamic tubulation of mitochondria from wild-type MEFs gives rise to a network *in vitro* (Figure 6I and Supplementary information, Movie S23). Thus, mitofusin-mediated fusion appears to be essential for connecting the dynamic tubules into a network. In agreement with this conclusion, adding GTP, which is required for activating mitofusin, greatly enhance the network formation (Supplementary information, Figure S12 and Movie S24), further supporting the role of mitofusin-mediated fusion in KIF5B-mediated network formation.

## Discussion

So far, fusion, fission and movement of mitochondria are established as the basic mechanisms for maintaining

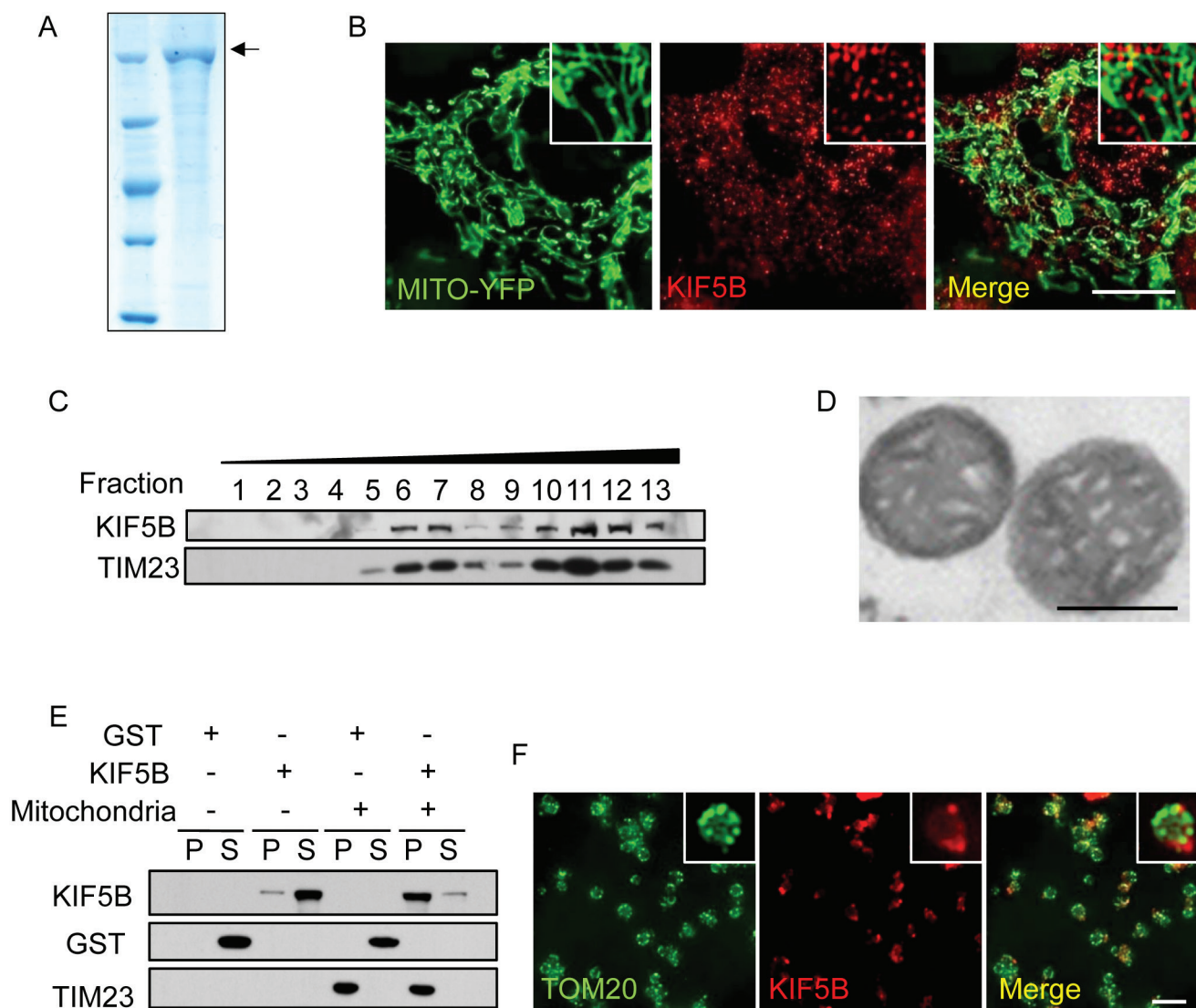
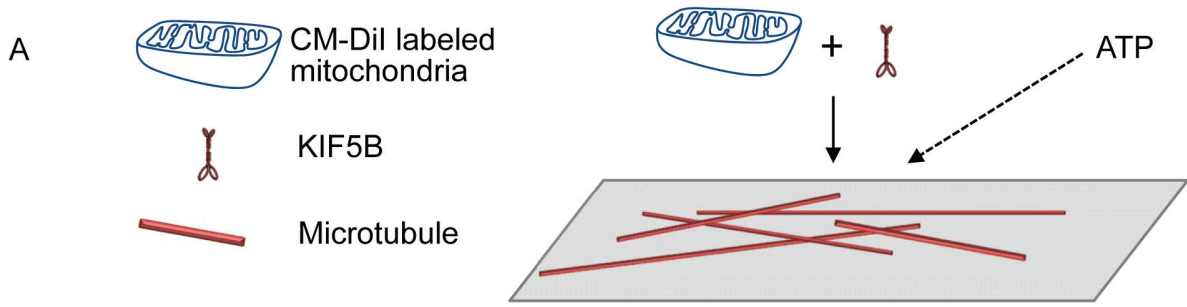


**Figure 4** KIF5B binds mitochondria *in vivo* and *in vitro*. **(A)** Analysis of purified full-length KIF5B by Coomassie staining. Black arrow indicates KIF5B protein. **(B)** NRK cells stably expressing Mito-YFP were treated with 25  $\mu\text{g/ml}$  digitonin and stained with antibodies against KIF5B. Scale bar, 10  $\mu\text{m}$ . **(C)** NRK cells were homogenized and centrifuged in OptiPrep density gradient medium. The distribution of KIF5B and the mitochondrial marker TIM23 in the fractions was monitored by western blotting. **(D)** TEM analysis of purified mitochondria from rat liver. Scale bar, 0.5  $\mu\text{m}$ . **(E)** Purified mitochondria were incubated with full-length KIF5B or GST, washed, and analyzed by western blotting with antibodies against KIF5B, GST and TIM23. **(F)** Purified mitochondria were incubated with Atto550-labeled KIF5B, and then stained with antibody against TOM20. Scale bar, 5  $\mu\text{m}$ .

mitochondrial dynamics and morphology. In this study, we demonstrate that KIF5B-mediated mitochondrial tubulation is an additional mechanism for regulating mitochondrial morphology. Based on these findings, we propose a modified model for mitochondrial network formation. In this model, dynamic tubulation of mitochondria, driven by KIF5B, gives rise to highly dynamic thin tubules, and mitofusin-mediated fusion of these tubules forms lattices which eventually interconnect to generate the mitochondrial network.

This model can explain phenomena in mitochondrial dynamics that are hard to understand based on the traditional fusion/fission model. For example, mitochondria can form branches by outgrowth of new tubules from existing mitochondrial tubes. The appearance of branches cannot be easily explained by fusion of mitochondria, but can be reasonably explained by kinesin-driven tubulation. Another example is the considerable variation in mitochondrial diameter, which again is difficult to explain by the current model but can be interpreted as a



**B**

Microtubules	-	-	+	+	+	+	+	+	+
KIF5B	+	+	-	-	+	+	-	-	+
KIF5B T92N	-	-	-	-	-	-	+	+	-
ATP	-	+	-	+	-	+	-	+	-
AMP-PNP	-	-	-	-	-	-	-	-	+
Mitochondria	+	+	+	+	+	+	+	+	+

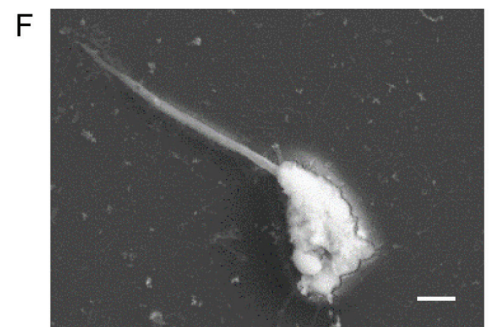
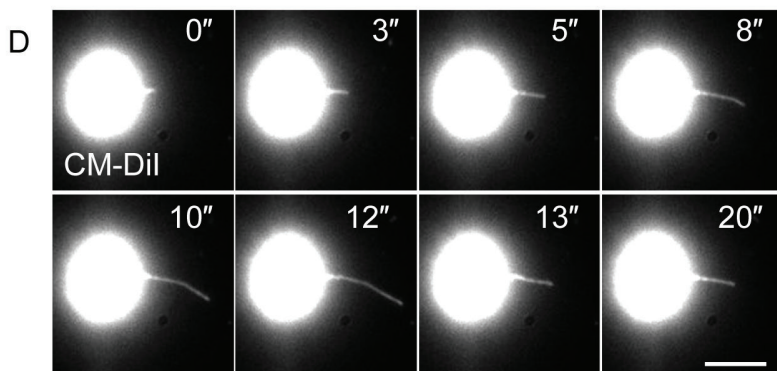
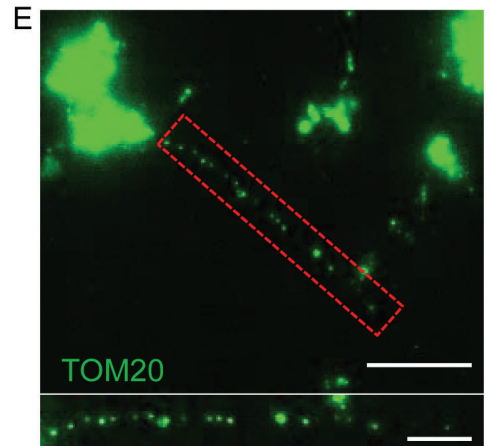
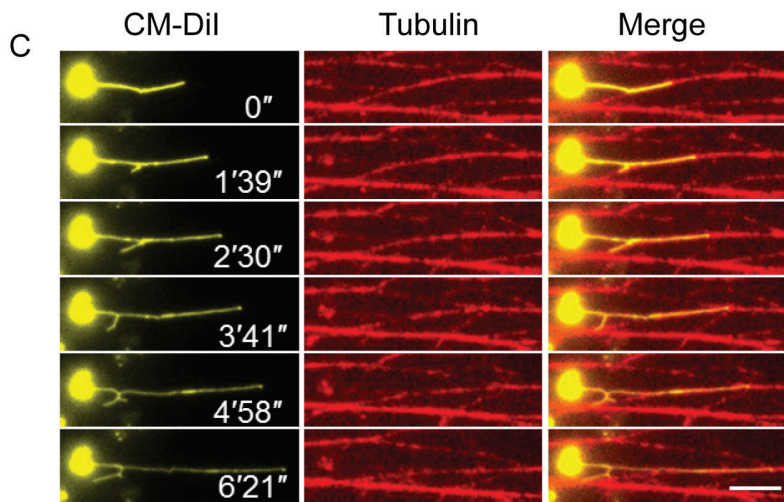


**Figure 5** KIF5B drives mitochondrial tubulation *in vitro*. **(A)** Schematic diagram of *in vitro* mitochondrial tubulation. Purified mitochondria were incubated with full-length KIF5B on ice, transferred into flow chamber channels coated with polymerized microtubules and visualized in the presence of ATP. **(B)** Purified mitochondria were labeled with CM-Dil, incubated with KIF5B, transferred into flow chamber channels coated with polymerized microtubules, and visualized in the presence of ATP. Several controls were carried out to test the requirement for each component. Scale bar, 5  $\mu\text{m}$ . **(C)** Time-lapse sequence of mitochondrial tubulation in the presence of ATP. Mitochondria were labeled with CM-Dil and microtubules were labeled with HyLite 647. Scale bar, 5  $\mu\text{m}$ . **(D)** Time-lapse sequence of mitochondrial tubulation in the presence of ATP. Scale bar, 5  $\mu\text{m}$ . **(E)** Samples from **B** were stained with antibody against TOM20, and observed by confocal microscopy. Scale bar, 10  $\mu\text{m}$ . Red dashed box is enlarged in the lower panel. Scale bar in enlarged panel, 5  $\mu\text{m}$ . **(F)** Samples from **B** were analyzed by FEISEM. Scale bar, 1  $\mu\text{m}$ .

kinesin-driven membrane deformation process. It will be interesting to test the role of kinesin in these phenomena in future work.

Our data demonstrate that KIF5B-mediated dynamic tubulation of mitochondria is an essential mechanism for formation of mitochondrial networks in the peripheral zone of cells. In KIF5B-knockout cells, the peripheral zones of the cells are devoid of mitochondria, whereas the mitochondrial network in the perinuclear zone is intact. This observation raises the interesting question of how the “inner” mitochondrial network is generated and maintained. It will be interesting to test whether other motor proteins or proteins that are capable of promoting tubule formation, such as some mitochondrial dynamin-related proteins [18, 19], play a role in formation of the “inner” mitochondrial network like KIF5B in the “outer” mitochondrial network.

## Materials and Methods

### *Antibodies, chemicals, and plasmids*

All chemicals were purchased from Sigma-Aldrich except GTP (BST06-001) and Taxol (TXD01), which were purchased from Cytoskeleton. Anti-actin (A2066) antibody was from Sigma-Aldrich. Anti-TIM23 (611222) and anti-TOM20 (612278) antibodies were from BD Biosciences. Anti-GST (ab19256), anti-KIF5B (ab167429), anti-Mitofusin 1 (ab57602), anti-Mitofusin 2 (ab56889), and anti-tubulin antibodies were from Abcam. HTS tubulin (HTS03-A1) was obtained from Cytoskeleton. Mito-YFP plasmid was constructed by fusing the mitochondrial target sequence of human COX8A with the YFP sequence. Mito-DsRed plasmid, a gift from Dr Chen Quan (Institute of Zoology, CAS), was constructed by fusing the mitochondrial target sequence of human TXN2 with the DsRed sequence. TOM20-GFP and TOM20-PAGFP were obtained by inserting the rat TOM20 coding sequence into pEGFP-N1 and PAGFP-N1, respectively. Tubulin-YFP was a gift from Dr Jennifer Lippincott-Schwartz (National Institute of Health).

### *Cell culture and transfection*

Cells were obtained from the American Type Culture Collection (ATCC), except MEF cells, which were a gift from Dr Chen Quan and originally from David Chan’s Research Group [6] (Division of Biology and the Howard Hughes Medical Institute, California

Institute of Technology, USA). Cells were cultured in DMEM (Life Technologies) supplemented with 10% FBS, 5% CO<sub>2</sub>, glutamax and penicillin-streptomycin. Cells were transfected with  $\leq 5 \mu\text{g}$  DNA via an AmaxaNucleofector II using solution T (for NRK cells) or a MEF2 kit (for all other cells) and programs for each cell line individually. Transfected cells were then cultured in growth medium for further analysis.

### *Generation of NRK cells with stable knockout of KIF5B*

The CRISPR/Cas9 system was a gift from Dr Wensheng Wei (Peking University). The sgRNA-binding sequence (5'-GTA-AACTTCATGATCCAGA-3') was used for KIF5B disruption with the CRISPR/Cas9 system. Cas9, gRNA and puromycin plasmid were co-transfected into NRK cells. Cells were cultured in medium containing puromycin for about 10 days, after which cell clones were picked and transferred into 96-well plates for amplification and analysis by western blotting and DNA sequencing.

### *Generation of NRK cells with tetracycline-inducible expression of KIF5B*

The KIF5B TET-ON inducible expression cell clone was generated with the T-REx™ system (K1020-01, Life Technologies) according to the manufacturer’s manual. The pcDNA™6/TR plasmid and KIF5B inducible expression construct were co-transfected at a ratio of 6:1 (w:w) into KIF5B-knockout NRK cells that stably express Mito-YFP. Antibiotic selection was carried out using 3  $\mu\text{g}/\text{ml}$  blasticidin and 100  $\mu\text{g}/\text{ml}$  Zeocin.

### *Statistics*

The Photoshop lasso tool was used to measure the percentage of the cytoplasmic area occupied by the mitochondria. The percentage was calculated as follows:  $\text{area occupied by mitochondria} / (\text{area of the cell} - \text{area of the nucleus}) \times 100\%$ . To calculate the ratio of the diameter of normal mitochondrial tubules to the diameter of dynamic tubules, 20 cells were imaged in each experiment of three, and a pair of tubules (one normal mitochondrial tubule and one dynamic tubule) was cropped from the same picture (Supplementary information, Figure S13). Using diameter measurement software developed by Yichen Zhou, the diameter of each tubule was determined at every pixel along the midline of the tubule. The average of these values was calculated to give the tube’s diameter. To determine the tubule diameter ratio for that cell, the diameter of the dynamic tubule was divided by the diameter of the normal mitochondrial tubule. Besides, we also measured diameter of mitochondrial tubules in EM image (Supplementary information, Figure S14), we measured the diameters of mitochondrial body and tube along the direction of tube (yellow line), and the maximum

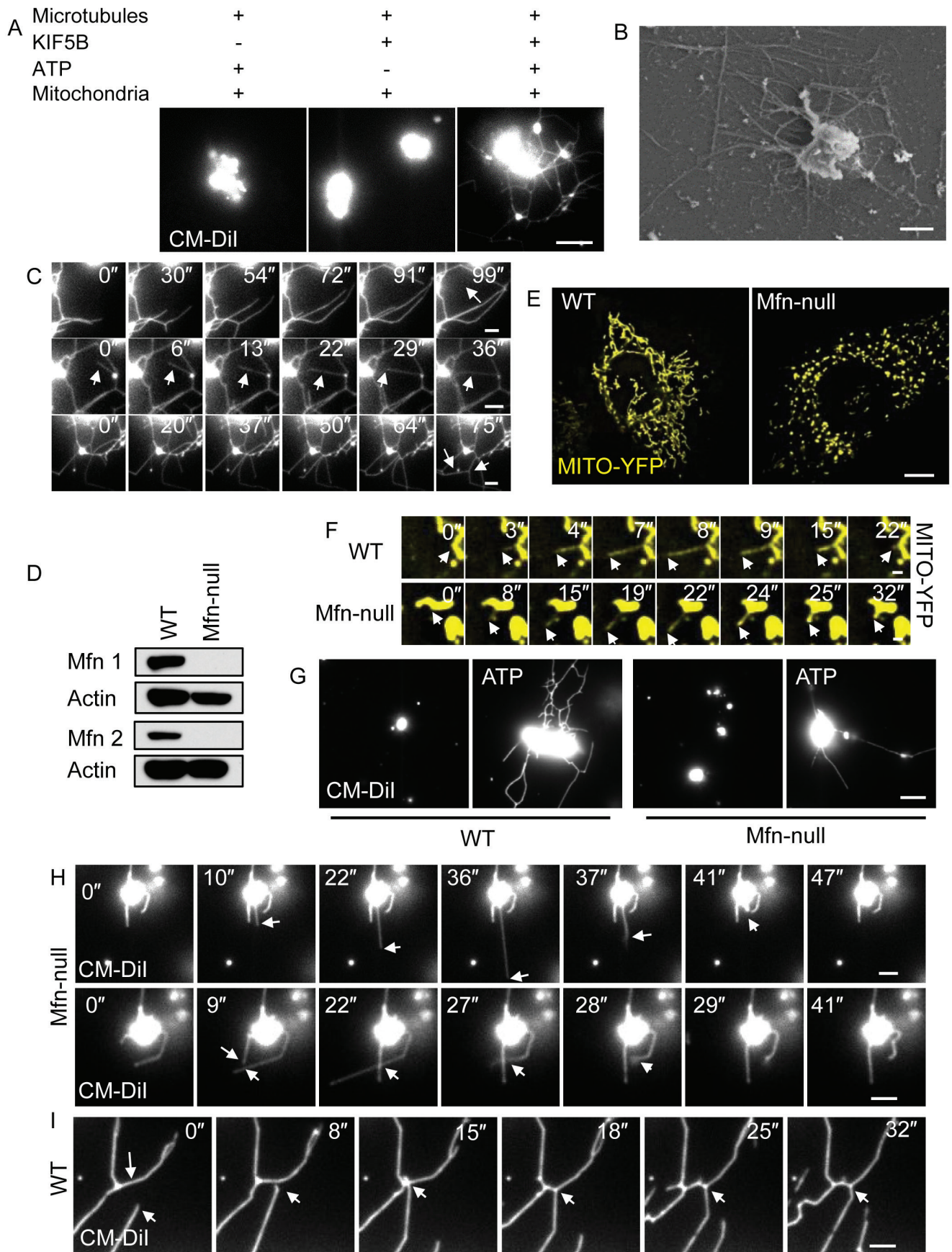


**Figure 6** KIF5B and mitofusins drive mitochondrial network reformation *in vitro*. **(A)** Purified mitochondria were labeled with CM-Dil. Highly concentrated mitochondria were incubated with KIF5B, transferred into flow chamber channels coated with polymerized microtubules, and visualized in the presence of ATP. Images were collected with a TIRF microscope. Scale bar, 5  $\mu\text{m}$ . **(B)** Samples from **A** were analyzed by FEISEM. Scale bar, 1  $\mu\text{m}$ . **(C)** Time-lapse sequence of **A**. Scale bar, 2  $\mu\text{m}$ . White arrows indicate newly formed lattices (top and bottom rows) or a tubule that divides a lattice (middle row). **(D)** Mfn1 and Mfn2 levels in Mfn-null MEF cells and wild-type (WT) MEF cells as shown by western blotting. **(E)** WT MEF cells and Mfn-null MEF cells were transfected with Mito-YFP and observed by spinning-disk microscopy. Scale bar, 10  $\mu\text{m}$ . **(F)** Time-lapse sequence of mitochondrial dynamic tubulation in WT (top row) and Mfn-null MEF cells (bottom row). Scale bar, 1  $\mu\text{m}$ . **(G)** Mitochondria from WT and Mfn-null MEF cells were tested in the *in vitro* reconstitution system for their ability to form mitochondrial networks. Scale bar, 5  $\mu\text{m}$ . **(H)** Time-lapse sequence of tubulation of mitochondria from Mfn-null MEF cells. Scale bar, 2  $\mu\text{m}$ . White arrows indicate pull-back of an unstable dynamic tubule (top row) or two crossed tubules that cannot fuse with each other (bottom row). **(I)** Time-lapse sequence of tubulation of mitochondria from WT MEF cells. Scale bar, 2  $\mu\text{m}$ . White arrows indicate a fusion event.

diameters (red and green arrows) were taken as final diameters. For *in vitro* network formation statistics, a tubular structure system that contains a closed loop was considered to be a network. For statistics of duration of tubulation events, the start of tubulation was defined by the appearance of a dynamic tubule. The end of tubulation was defined by four events: (1) tubules retracted into the mitochondrial body, (2) tubules fused with other mitochondria, (3) tubules stopped growing, and (4) tubules broke away. The duration of tubulation was defined as the time between the start and end of a dynamic tubulation event.

#### Mitochondrial purification

Mitochondrial purification was performed with some modifications as described previously [15]. Rat liver (2 g) or 20 dishes (15 cm) of cultured cells were washed with PBS several times, homogenized with a Dounce homogenizer in 4 ml of H-S buffer (10 mM HEPES, pH 7.4, 320 mM sucrose, 5 mM  $\text{MgSO}_4$ , 1 mM EGTA, 1 mM DTT, and protease inhibitors), and centrifuged at 1 000 $\times$   $g$  for 10 min at 4  $^\circ\text{C}$ . The pellet was discarded and the supernatant was centrifuged at 11 400 $\times$   $g$  for 20 min at 4  $^\circ\text{C}$ . The pellet was resuspended in 500  $\mu\text{l}$  H-S buffer and applied on the top of a HEPES-buffered sucrose step density gradient (0.3 ml of 2.3 M, 1.7 ml of 1.7 M, and 1.5 ml of 1 M). The gradient was centrifuged at 100 000 $\times$   $g$  for 30 min at 4  $^\circ\text{C}$ . 500  $\mu\text{l}$  of 1 M/1.7 M interface was recovered, diluted 3-fold with H-S buffer, and pelleted by centrifuging for 10 min at 11 400 $\times$   $g$ . This wash step was repeated 3 times.

#### Flow chamber

The flow chamber (containing four individual channels) used for the *in vitro* reconstitution assay was home-made from coverslips (12-545-F, Thermo Fisher, USA) and slides (10127101P, Shitai, Jiangsu, China). Double-sided tape (200 MP, 3M (Minnesota Mining and Manufacturing), USA) was used to stick the coverslip and slide together and to isolate the flow channels. The coverslips were cleaned in acetone (Guoyao, China) followed by 1 M KOH (484016, Sigma-Aldrich, USA) with sonication (KQ500DE, Kunshan, China) and stored in ddH<sub>2</sub>O to keep the surface hydrophilic.

#### Staining and imaging

Cells were washed in PBS, permeabilized in 25  $\mu\text{g}/\text{ml}$  digitonin for 5 min, and fixed in 4% paraformaldehyde for 10 min. Fixed cells were blocked with 10% FBS in PBS for 30 min, stained with 10  $\mu\text{g}/\text{ml}$  of antibody in blocking buffer for 1 h, and washed with PBS. Cells were then stained with secondary antibody in blocking

buffer for 1 h and washed with PBS three times.

To detect KIF5B on mitochondria, purified mitochondria were incubated with Atto550-labeled KIF5B, transferred into flow chambers, fixed and stained with antibodies.

For live-cell imaging, transfected cells were replated in Lab-Tek chambered coverglasses before imaging, and cells were maintained at 37  $^\circ\text{C}$  with 5% CO<sub>2</sub>. Images were acquired using an Olympus FV-1000 confocal microscope. Videos were acquired on a PerkinElmer UltraViewVox spinning-disk microscope system. SIM images were acquired on an N-SIM using a 100 $\times$  oil immersion lens (numerical aperture 1.49).

#### Cell fractionation assay

Two dishes (15 cm) of NRK cells were homogenized with a Dounce homogenizer in extraction buffer containing protease inhibitor cocktail. The homogenate was diluted with 19% Optiprep density gradient medium solution, and overlaid with 30%, 25%, 15%, 12%, 10%, 8%, 5%, and 2% Optiprep solutions. After centrifugation at 150 000 $\times$   $g$  for 4 h, the fractions were collected and analyzed by western blotting.

#### Protein expression, purification and labeling

pFastBac DUAL was used as a vector for baculovirus expression. This vector does not contain a tag for purification, thus a histidine ( $\times 6$ ) tag was introduced before the first codon of full-length KIF5B. The histidine-tagged KIF5B coding sequence was cloned between the *Bam*H I/*Xba* I sites of the pFastBac DUAL plasmid. Full-length KIF5B protein was expressed using the Bacto-Bac expression system. Sf9 cells were grown in Lonza media to a density of  $\sim 2 \times 10^6$  cells/ml and incubated with virus containing full-length KIF5B construct. After 60 h, cells were collected, lysed by freeze-thaw cycles, and centrifuged at 4  $^\circ\text{C}$ . The soluble fraction was bound in batches to Ni-NTA agarose, and the resin was washed. His6-tagged KIF5B was eluted with 20 mM Tris, 0.1 M NaCl, 250 mM imidazole, pH 8.0. The eluate was concentrated and stored in 50  $\mu\text{M}$  HEPES-KOH, pH 7.4, 300 mM NaCl, 1 mM  $\text{MgCl}_2$ , 10% (w/v) sucrose and 50  $\mu\text{M}$  ATP. KIF5B was labeled with Atto550, a monofunctional NHS ester that labels free amino groups, for 30 min on ice. KIF5B-Atto550 was removed from free dye by gel filtration using a NAP5 column.

#### Gliding assays

The gliding assay chambers were prepared by using hydrophilic coverslips. 15  $\mu\text{l}$  of full-length KIF5B were incubated in flow chamber channels for 5 min. The kinesin-coated coverslips were

blocked with 3 mg/ml casein for 5 min, and then 40 nM of HyLite 647-labeled microtubules was introduced into the flow chamber. An ATP solution containing 0.5 mM ATP, 20  $\mu$ M taxol, 10 mM DTT, 1 mg/ml casein, an ATP regeneration system, and an oxygen scavenger system were subsequently added to the chamber. Images were recorded every 0.5 s using a Nikon Ti-E TIRF microscope under 640-nm laser excitation.

#### *In vitro* reconstitution of mitochondrial tubulation

The tubulation assay chambers were prepared as for the gliding assay. The channels were sequentially coated with 10  $\mu$ g/ml anti-tubulin antibody and 3 mg/ml casein, allowing microtubules to be immobilized on the coverslips. Full-length KIF5B (80 nM) was incubated with  $\sim$ 0.4 mg/ml mitochondria. The motor-coated mitochondria were introduced into the microtubule-coated flow chambers, and then 60  $\mu$ l of ATP solution containing 20  $\mu$ M ATP, 20  $\mu$ M taxol, 1 mg/ml casein, an ATP regeneration system, and an oxygen scavenger system were added to the chambers. The formation of tubes was visualized using a Nikon TIRF microscope.

#### FEISEM

For field emission in-lens scanning electron microscopy (FEISEM), tubulated mitochondria were incubated on glass chips at 37 °C for 1 h, and then fixed with 2% glutaraldehyde in PBS buffer at room temperature for 30 min. The samples were then rinsed and post-fixed with 1.0% OsO<sub>4</sub> in 0.1 M sodium cacodylate buffer at room temperature for 20 min. After dehydration in a graded ethanol series (30%, 50%, 70%, 90%, 100%, and 100%, 10 min each), the samples were transferred to Arklone for critical-point drying using highest-purity CO<sub>2</sub> in a Hitachi HCP-2 Critical Point Dryer. The samples were then coated with 4 nm gold in a Hitachi E-1045 ion sputter coater and viewed in a Hitachi scanning electron microscope S4800 at a 6 kV accelerating voltage.

#### Acknowledgments

We are grateful to Tsinghua-Nikon imaging center and Tsinghua Imaging Core Facility for providing technical support, and to Yanli Zhang, Xuan Tang and Jinyu Wang for assistance with confocal microscopy and image processing. We thank Dr Quan Chen for providing reagents. This research was supported by the National Natural Science Foundation of China (31123004, 31030043, 30971484 and 31321003), and the National Basic Research Program of China (973 Program; 2011CB910100).

#### References

- Chan DC. Fusion and fission: interlinked processes critical for mitochondrial health. *Annu Rev Genet* 2012; **46**:265-287.
- Chen H, Chan DC. Mitochondrial dynamics--fusion, fission, movement, and mitophagy--in neurodegenerative diseases. *Hum Mol Genet* 2009; **18**:R169-R176.
- Nunnari J, Marshall WF, Straight A, Murray A, Sedat JW, Walter P. Mitochondrial transmission during mating in *Saccharomyces cerevisiae* is determined by mitochondrial fusion and fission and the intramitochondrial segregation of mitochondrial DNA. *Mol Biol Cell* 1997; **8**:1233-1242.
- Mishra P, Chan DC. Mitochondrial dynamics and inheritance during cell division, development and disease. *Nat Rev Mol*

- Cell Biol* 2014; **15**:634-646.
- Bleazard W, McCaffery JM, King EJ, *et al.* The dynamin-related GTPase Dnm1 regulates mitochondrial fission in yeast. *Nat Cell Biol* 1999; **1**:298-304.
- Chen H, Detmer SA, Ewald AJ, Griffin EE, Fraser SE, Chan DC. Mitofusins Mfn1 and Mfn2 coordinately regulate mitochondrial fusion and are essential for embryonic development. *J Cell Biol* 2003; **160**:189-200.
- Sesaki H, Jensen RE. Division versus fusion: Dnm1p and Fzo1p antagonistically regulate mitochondrial shape. *J Cell Biol* 1999; **147**:699-706.
- Smirnova E, Griparic L, Shurland DL, van der Bliek AM. Dynamin-related protein Drp1 is required for mitochondrial division in mammalian cells. *Mol Biol Cell* 2001; **12**:2245-2256.
- Rojo M, Legros F, Chateau D, Lombes A. Membrane topology and mitochondrial targeting of mitofusins, ubiquitous mammalian homologs of the transmembrane GTPase Fzo. *J Cell Sci* 2002; **115**:1663-1674.
- Santel A, Fuller MT. Control of mitochondrial morphology by a human mitofusin. *J Cell Sci* 2001; **114**:867-874.
- Meeusen S, McCaffery JM, Nunnari J. Mitochondrial fusion intermediates revealed *in vitro*. *Science* 2004; **305**:1747-1752.
- Vale RD, Reese TS, Sheetz MP. Identification of a novel force-generating protein, kinesin, involved in microtubule-based motility. *Cell* 1985; **42**:39-50.
- Vale RD, Hotani H. Formation of membrane networks *in vitro* by kinesin-driven microtubule movement. *J Cell Biol* 1988; **107**:2233-2241.
- Dabora SL, Sheetz MP. The microtubule-dependent formation of a tubulovesicular network with characteristics of the ER from cultured cell extracts. *Cell* 1988; **54**:27-35.
- Tanaka Y, Kanai Y, Okada Y, *et al.* Targeted disruption of mouse conventional kinesin heavy chain, kif5B, results in abnormal perinuclear clustering of mitochondria. *Cell* 1998; **93**:1147-1158.
- Huang X, Sun L, Ji S, *et al.* Kissing and nanotunneling mediate intermitochondrial communication in the heart. *Proc Natl Acad Sci USA* 2013; **110**:2846-2851.
- Sehgal L, Mukhopadhyay A, Rajan A, *et al.* 14-3-3gamma-mediated transport of plakoglobin to the cell border is required for the initiation of desmosome assembly *in vitro* and *in vivo*. *J Cell Sci* 2014; **127**:2174-2188.
- Ban T, Heymann JA, Song Z, Hinshaw JE, Chan DC. OPA1 disease alleles causing dominant optic atrophy have defects in cardiolipin-stimulated GTP hydrolysis and membrane tubulation. *Hum Mol Genet* 2010; **19**:2113-2122.
- Mears JA, Lackner LL, Fang S, Ingerman E, Nunnari J, Hinshaw JE. Conformational changes in Dnm1 support a contractile mechanism for mitochondrial fission. *Nat Struct Mol Biol* 2011; **18**:20-26.

(Supplementary information is linked to the online version of the paper on the *Cell Research* website.)



This work is licensed under the Creative Commons Attribution-NonCommercial-No Derivative Works 3.0 Unported License. To view a copy of this license, visit <http://creativecommons.org/licenses/by-nc-nd/3.0>